Clays and Clay Minerals, Vol. 64, No. 6, 743–752, 2016.

INTERACTION OF MAGNESIUM CATIONS WITH DIOCTAHEDRAL SMECTITES UNDER HLRW REPOSITORY CONDITIONS

S. Kaufhold[1,*], R. Dohrmann[1,2], and K. Ufer[1]

[1]BGR, Bundesanstalt für Geowissenschaften und Rohstoffe, Stilleweg 2, D-30655 Hannover, Germany
[2]LBEG, Landesamt für Bergbau, Energie und Geologie, Stilleweg 2, D-30655 Hannover, Germany

Abstract—In some real and up-scale tests using high-level radioactive waste (HLRW), Mg accumulation was observed in smectites at the contact of heated Fe or Cu metal tubes. It is important to understand why Mg accumulated in order to model the long term performance of bentonites in HLRW systems. In some of these tests, an increased number of trioctahedral domains was measured in the smectites using X-ray diffraction (XRD) and infrared spectroscopy (IR). The trioctahedral domains either formed by the dissolution/precipitation of smectites or by the addition of Mg through a solid-state reaction similar to the Hofmann-Klemen effect. The Hofmann-Klemen effect is used in the Greene-Kelly test to distinguish montmorillonites from beidellites. Many studies have been carried out about Li-uptake by smectites, but Mg was rarely taken into account. The present study was, therefore, undertaken to compare the interactions of different bentonites with Li and Mg under various conditions. A significant CEC decrease was found for Li- and Mg-saturated bentonite samples after heating at 250ºC under dry conditions. The extent of this CEC reduction depended on the octahedral to tetrahedral charge ratio and was smaller for Mg-saturated samples than Li-saturated samples. This finding proved that it is much more difficult for Mg to enter octahedral vacancies than Li, which probably can be explained by the larger hydration energy and/or slightly larger radius of Mg. The relationship between CEC reduction and the octahedral/tetrahedral charge ratio of both Li- and Mg-saturated samples, however, suggests a similar process. The Mg that can reside at the bottom of the pseudohexagonal holes would not explain this relationship. The important result with respect to understanding HLRW bentonite performance, on the other hand, is that Mg fixation only occurs under dry conditions and that Mg fixation acts as a sink for Mg and, hence, leads Mg to diffuse towards the heated metal surface.

Key Words—Dioctahedral to Trioctahedral Transformation, HLRW Bentonite, Mg-increase, Smectite, Trioctahedral Domains.

INTRODUCTION

Swelling clays (smectite rich clays or bentonites) are currently investigated as potential geotechnical barriers for the safe encapsulation of high level radioactive waste (HLRW) (Dohrmann *et al.*, 2013a; Sellin and Leupin, 2014, Kaufhold and Dohrmann, 2016). The current focus is on the identification of mineral alteration reactions, which could affect the long term performance of bentonite barriers. Among other reactions, the accumulation of Mg in bentonites exposed to a heated metal surface was found in some large and/or up-scale tests. Neither the reason for this Mg accumulation nor the mechanism behind it are currently understood. For safety assessments, the long term performance of the barrier must be investigated. Long term performance assessment is commonly based on modelling because of the marked difference between the age of deposition tests (1−10 y) and safety requirements (up to 1 Ma). Reasonable modeling, however, can only be based on understanding the mechanisms of the smectite alteration processes as these minerals guarantee the most important safety functions. Such alteration processes were observed particularly at metal-bentonite and cement-bentonite interfaces. The high pH at cement-bentonite interfaces results in dissolution of smectites and precipitation of zeolites and related minerals (*e.g.* Savage *et al.*, 1992, 2010). At metal-bentonite interfaces, corrosion products, such as 1:1 or 2:1 minerals, were observed after all the oxygen was consumed during magnetite formation (Perronnet *et al*., 2007; Savage *et al*., 2010; Kaufhold *et al*., 2015). Some large scale tests, however, indicated the relevance of an additional alteration mechanism. At and near metal-bentonite interfaces, an enrichment of Mg was observed which could not be explained by cation exchange only. Detailed mineralogical analysis revealed the formation of trioctahedral minerals and/or domains. Such a dioctahedral to trioctahedral transformation mostly occurred along with an increase in the Mg content and was observed in a couple of HLRW large scale tests at both Cu-metal/bentonite and Fe-metal/bentonite interfaces (long term test, LOT: Kaufhold and Dohrmann, 2009; alternative buffer material test, ABM-I: Kaufhold *et al*., 2013; Dohrmann and Kaufhold, 2013b; ABM-II: Svensson, 2015). Plötze *et al.* (2007) reported on the increase in Mg contents in bentonite that was observed in the Mont Terri heater

* E-mail address of corresponding author:
s.kaufhold@bgr.de
DOI: 10.1346/CCMN.2016.064041

experiment (HE-B) in the Opalinus clay formation, Switzerland. In the low-temperature, full-scale experiment, prototype repository (Cu-metal/bentonite interfaces) test, no trioctahedral domains were found (Dohrmann and Kaufhold, 2014). In the ABM tests, only a few bentonites showed a dioctahedral to trioctahedral transformation of smectites. Tests with other materials showed no alteration, no Mg increase, and no increase in trioctahedral minerals or domains and cannot yet be explained. The formation mechanism for trioctahedral minerals and/or domains, hence, is not yet understood. The aim of the present paper, therefore, was to investigate the interaction of smectites with excess Mg at elevated temperature.

The Mg that sometimes accumulated near the heater/bentonite interface can be derived from (1) cation exchange, (2) ground or rock water, (3) incongruent smectite dissolution, or (4) a combination of all three processes. The Mg source is not clear, but the occurrence of trioctahedral minerals or domains at heater/bentonite contacts has been proven.

Two different mechanisms for the formation of trioctahedral domains have to be taken into account. On the one hand, the formation of trioctahedral minerals or domains could be explained by dissolution of a dioctahedral smectite and precipitation of a trioctahedral smectite. This reaction would depend on the solubility of the precursor material and the Mg abundance. On the other hand, a dioctahedral to trioctahedral transformation could be a solid state "addition" reaction. Analogous to the fixation of Li by dioctahedral smectites (Greene-Kelly, 1952; Hofmann and Klemen, 1950), Mg has only a slightly larger ionic radius than Li and could enter octahedral vacancies in smectites and partially neutralize the permanent layer charge. The fixation of Li is used to distinguish montmorillonites from beidellites. Some doubt, nevertheless, exists about the actual fixation process. Most IR-based methods have proved the presence of Li in octahedral vacancies (*e.g.* Madejová *et al.*, 2000). NMR studies, on the other hand, indicate that Li remains at the bottom of the pseudohexagonal holes (Steudel *et al*., 2015). Most studies agree that Li can migrate into octahedral vacancies most probably near the permanent charges (Sasra *et al*., 1994; Karakassides *et al*., 1999; Hrobáriková *et al*., 2001). The presence of Li in octahedral vacancies near layer charge sites was also found to be energetically favorable (Stackhouse and Coveney, 2002). No such studies, however, are available for Mg. A few studies were conducted on the fixation of small bivalent cations, such as Cu. Madejová *et al*. (1999) concluded that Cu remains at the bottom of the hexagonal holes and that not only size but also the charge and hydration energy determine the fate of the cations in the mineral structure. Li fixation by smectites and Mg fixation by hectorite was studied by Jaynes and Bigham (1987) and Jaynes *et al.* (1992). The present study was conducted to try to identify the reaction mechanism relevant for HLRW disposal. Fixation tests were, therefore, conducted on a set of bentonites that contain smectites with different ratios of octahedral and tetrahedral charge.

MATERIALS AND METHODS

Eight bentonites of the BGR bentonite sample set (Kaufhold and Dohrmann, 2008; Kaufhold *et al.*, 2008; Kaufhold *et al*., 2010a, 2010b) were selected. To avoid cation exchange processes caused by the dissolution of Ca-carbonate or Ca-sulfate during the experiments as discussed by Dohrmann (2006), samples with a low content of partially soluble components were selected. In addition, the samples covered a significant range of total layer charge densities and tetrahedral charge fraction of total charge because both could play a role in cation fixation. Basic mineralogical and chemical data of the samples is given in Table 1.

Mg-interaction experiments

For Li-saturation, a 5 g sample of each bentonite was dispersed in 750 mL polyethylene (PE) centrifuge beakers in 500 mL of a 4 M LiCl solution and were shaken end-over-end for 24 h. The bentonite solids were separated from the LiCl solution by centrifugation and were washed with deionized water. To complete Li saturation, a second aliquot of 500 mL of 4 M LiCl solution was added and was shaken end-over-end for another 24 h. After centrifugation and washing, the sedimented bentonite samples were dialyzed and either air-dried and ground or the volume was reduced to 10 mL by evaporation. The Mg-saturation was similar to the procedure described above for Li-saturation, but a 10 g sample of bentonite and a 4 M $MgCl_2$ solution were used. The experimental setup is summarized in Table 2. The CEC is commonly determined after drying samples at <100ºC and the CEC values are corrected using the water contents determined on separate samples dried at 105ºC. Drying at >100ºC may cause a reduction in the CEC (Kaufhold and Dohrmann, 2010a). In most of the series (Table 2), temperatures above 100ºC were applied and, therefore, the untreated material was also investigated after drying at 120ºC for 24 h. The standard procedure for Li-fixation is drying at 250ºC for a couple of hours. In a repository in crystalline rock, however, the temperature in the bentonite buffer will be <100ºC and, in large-scale experiments, ABM temperatures in the bentonite buffer can reach up to 135ºC. Additional tests were, therefore, conducted at 120ºC with an increased reaction time. In addition, the water content was assumed to play a role. Two tests, one without and one with water, were conducted. Li is known to enter the octahedral vacancies, but Mg movement was thought to be slower. Hence, the time for the Mg experiments was increased.

https://doi.org/10.1346/CCMN.2016.064041 Published online by Cambridge University Press

Table 1. Basic mineralogical and chemical parameters of the eight selected bentonite samples ("0" = mineral was detected, but content <0.5%).

		B2	B4	B14	B22	B29	B33	B36	B39
Mineral composition (%)		Kaufhold *et al*. (2012)							
Smectite		77	91	88	76	89	88	75	60
Muscovite		3							
Kaolinite				3		5		2	
Quartz		1	2	3	4	6	3	11	
Cristobalite/opal-A				12		1	3	40	
Rutile/anatase			1	2				0	
Calcite		0		1	0		1		
Feldspar		19	5	3	8	0	7	8	
Barite			1						
Gypsum							0		
Sum		100	100	100	100	100	100	100	100
BET		Kaufhold *et al*. (2010b)							
	(m^2/g)	22	46	130	31	96	16	57	111
Tetrahedral charge	(%/CEC)	13	23	60	7	31	12	51	55
Layer charge density (AAM)	(eq/FU)	0.35	0.31	0.33	0.35	0.33	0.25	0.20	n.d.
LECO		Kaufhold *et al*. (2008)							
C_{total}	(mass%)	0.1	0.0	0.2	0.0	0.1	0.1	0.1	0.0
C_{org}	(mass%)	0.0	0.0	0.1	0.0	0.1	0.1	0.1	0.0
C_{inorg}	(mass%)	0.0	0.0	0.1	0.0	0.0	0.1	0.0	0.0
S_{total}	(mass%)	0.0	0.1	0.0	0.0	0.0	0.0	0.0	0.0
CEC		Kaufhold and Dohrmann (2008)							
Na	(meq/100g)	13	19	1	66	0	57	0	2
K	(meq/100g)	2	2	3	1	1	2	2	1
Mg	(meq/100g)	47	46	41	3	23	5	17	11
Ca	(meq/100g)	42	38	48	27	44	33	36	45
Sum cations	(meq/100g)	104	105	93	97	68	97	54	59
CEC	(meq/100g)	102	107	86	98	77	81	53	59
XRF		Kaufhold and Dohrmann (2008)							
SiO_2	(mass%)	52.0	49.4	45.8	62.4	49.8	58.6	61.7	69.1
TiO_2	(mass%)	0.6	0.7	2.1	0.2	1.2	0.1	0.8	0.2
Al_2O_3	(mass%)	15.4	15.6	16.8	15.0	21.0	19.5	17.5	15.6
Fe_2O_3	(mass%)	5.0	8.0	9.9	1.1	5.4	3.6	8.1	1.9
MnO	(mass%)	0.1	0.0	0.0	0.0	0.0	0.0	0.1	0.0
MgO	(mass%)	4.4	3.1	2.2	3.3	1.9	2.4	1.6	0.6
CaO	(mass%)	1.7	0.9	1.6	1.0	1.1	1.2	1.3	1.3
Na_2O	(mass%)	0.9	0.6	0.1	2.3	0.0	2.1	0.4	0.0
K_2O	(mass%)	1.1	0.4	0.7	0.4	0.1	0.5	1.4	0.2
P_2O_5	(mass%)	0.1	0.1	0.4	0.1	0.0	0.0	0.1	0.0
LOI	(mass%)	18.5	19.5	20.3	13.9	19.3	11.4	6.7	10.9
Sum	(mass%)	99.6	98.7	99.6	99.8	99.7	99.7	99.7	99.8

Analysis of products

The products were analyzed using X-ray diffraction (XRD) with attention to the d_{060} reflection, using infrared spectroscopy (IR) with attention to the 680 cm^{-1} vibration, and by using cation exchange capacity (CEC) to determine any loss in CEC that would suggest cation fixation.

The XRD patterns were recorded using a PANalytical X'Pert PRO MPD θ-θ diffractometer (PANalytical, Almelo, Netherlands) using Cu-Kα radiation generated at 40 kV and 30 mA and was equipped with a variable divergence slit (20 mm irradiated length), primary and secondary soller slits, a proportional counter, a diffracted-beam monochromator, and a sample changer (sample diameter 28 mm). The samples were investi-

https://doi.org/10.1346/CCMN.2016.064041 Published online by Cambridge University Press

Table 2. Experimental setup used for Li and Mg interaction tests using 8 selected bentonites.

	Samples				(ºC)	(h)
Series 1	8 selected bentonites	Untreated material, natural cation population, dried			120	24
Series 2	8 selected bentonites	Li saturated	dialysed	dried	250	4
Series 3	8 selected bentonites	Li saturated	dialysed	dried	120	24
Series 4	8 selected bentonites	Li saturated	dialysed	in 10 mL water	120	24
Series 5	8 selected bentonites	Mg saturated	dialysed	dried	250	24
Series 6	8 selected bentonites	Mg saturated	dialysed	dried	120	720
Series 7	8 selected bentonites	Mg saturated	dialysed	in 10 mL water	120	720

gated from 2º to 90º2θ using a step size of 0.02º2θ and a measuring time of 20 sec per step. For specimen preparation, the top loading technique was used.

For measuring the mid (MIR) infrared spectra, the KBr pellet technique (1 mg sample/200 mg KBr) was applied and spectra were collected using a Thermo Nicolet Nexus FTIR spectrometer (Nicolet Instruments, Madison, Wisconsin, USA) with a MIR beam splitter, KBr windows, and a DTGS TEC detector with the resolution adjusted to 2 cm^{-1}. Measurements were conducted before and after the KBr pellets were dried at 150ºC in a vacuum oven for 24 h. The CEC was measured using the Cu-triethylenetetramine (Cu-trien) method (Meier and Kahr, 1999; Dohrmann and Kaufhold, 2009).

RESULTS AND DISCUSSION

CEC after Li/Mg treatment

All CEC values are summarized in Table 3. The 60ºC reference CEC values (1st column Table 3) were taken from Kaufhold and Dohrmann (2008). The values were determined on 60ºC dried material and corrected for the water content from 60−105ºC. The CEC values of the series 1 samples (2nd column Table 3) were determined after pre-drying the samples of the present study at 120ºC for one day. The CEC values of the series 1 samples after 120ºC heating were expected to be lower than the values published by Kaufhold and Dohrmann (2008) that were determined on samples that were dried at 60ºC with the sample weights corrected for water loss. Obviously, the 120ºC heating led to a 10−20% reduction of the CEC. At least part of this CEC reduction can be explained by cation fixation (Kaufhold and Dohrmann, 2010a). After Li saturation and drying at 60ºC (after Li sat, 60ºC, Table 3), slightly lower CEC values were observed. In contrast, the CECs were slightly larger after Mg saturation and drying at 60ºC (after Mg sat, 60ºC, Table 3) and drying at 120ºC in comparison to samples from series 1 heated at 120ºC with a natural cation population (Table 3). This difference cannot be explained by the different pH values (Kaufhold *et al*., 2008).

Regardless of the actual reasons for the CEC decrease after Li/Mg saturation and drying at 60ºC, the CEC values after saturation with Li and Mg and drying at 60ºC were used as reference values for all Li experiments ("Li sat 60ºC") and for all Mg experiments ("Mg sat 60ºC") (Table 3, x-axis in Figure 1), respectively. These CEC values were compared with the samples heated to 120 and 250ºC, respectively. The Li samples heated to 120ºC (series 3) showed a slight CEC decrease after the 120ºC treatment, whereas no significant CEC

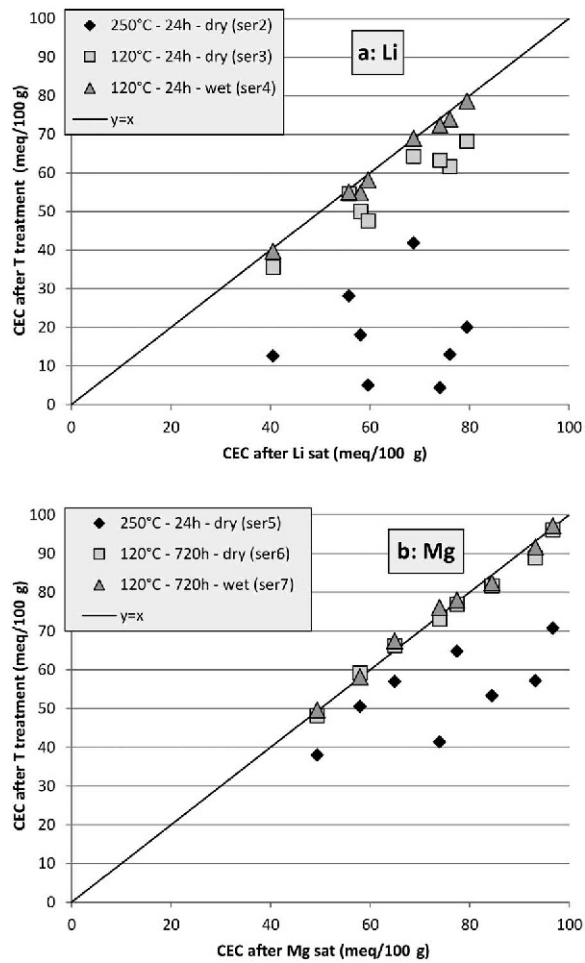

Figure 1. The CEC decrease for the Li-saturated (a: series 2-4, Table 2) and Mg-saturated (b: series 5-7, Table 2) bentonite samples after different temperature treatments.

https://doi.org/10.1346/CCMN.2016.064041 Published online by Cambridge University Press

Table 3. The CEC values (meq/100 g) of the untreated bentonites dried at 60ºC and 120ºC and the Li- and Mg-saturated bentonite samples heated to 120ºC or 250ºC where the "250/4/dry" label indicates heating at 250ºC/for 4 h/under dry conditions. Sample numbers B2, B4, B22, and B33 in bold print had the largest CEC reductions and lowest tetrahedral charge.

	Untreated 60ºC natural cation population (Table 1)	Series 1 (120ºC) untreated	After Li sat 60ºC	Series 2 Li sat 250/4/dry	Series 3 Li sat 120/24/dry	Series 4 Li sat 120/24/wet	After Mg sat 60ºC	Series 5 Mg sat 250/24/dry	Series 6 Mg sat 120/720/dry	Series 7 Mg sat 120/720/wet	ΔCEC, Li Li-250-dry Series 2	Δ CEC, Mg Mg-250-dry Series 5
B2	102	82	76	13	62	74	93	57	89	92	63	36
B4	107	93	80	20	68	79	97	71	96	97	59	26
B14	86	79	69	42	64	69	77	65	77	78	27	13
B22	98	79	74	4	63	72	84	53	82	82	70	31
B29	77	62	58	18	50	55	65	57	66	67	40	8
B33	81	72	60	5	48	58	74	41	73	76	55	33
B36	53	43	41	13	36	40	49	38	48	50	28	11
B39	59	53	56	28	55	55	58	50	59	58	28	7

decrease for the wet samples was observed (series 4, Figure 1a). After the 250ºC heating, all the Li samples showed a marked CEC decrease, which according to Greene-Kelly (1952) and Hofmann and Klemen (1950) can be explained by Li movement into the octahedral vacancies. The Mg-saturated samples heated to 120ºC did not show any CEC change, regardless of whether the samples were still suspended in water during heat treatment or dry, and despite the much longer heating time. After the 250ºC heating, however, a significant CEC decrease for the Mg-saturated samples heated to 250ºC was observed, but the CEC decrease still was less than that of the Li-saturated samples.

The extent to which the CEC of the Li-saturated samples decreased after 250ºC heating depended on the tetrahedral charge (Figure 2a). This was expected because

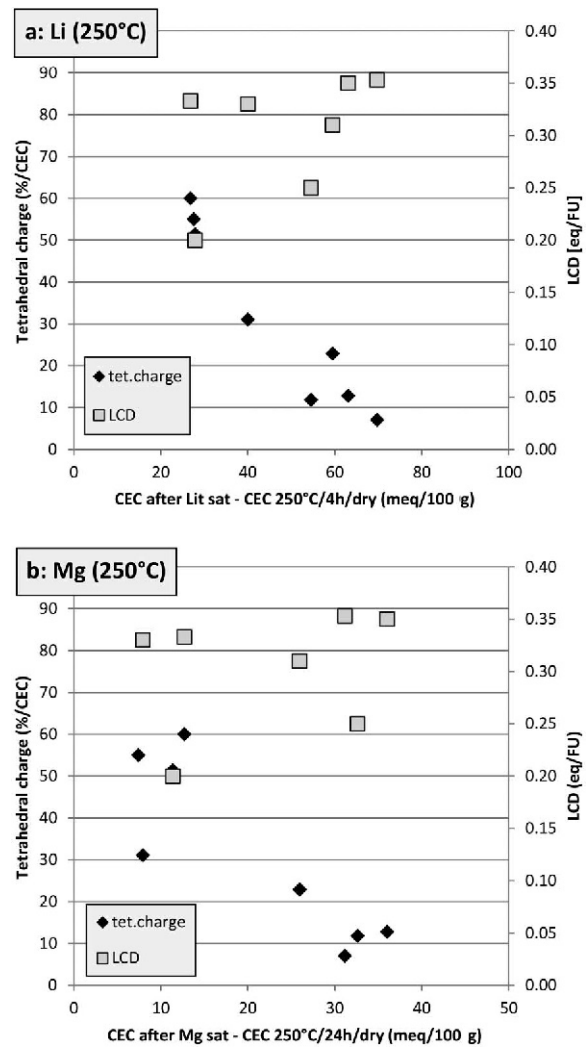

Figure 2. The CEC decrease for the Li-saturated (a: series 2, Table 2) and Mg-saturated (b: series 5, Table 2) and heat treated (250ºC, dry) bentonite samples compared to the tetrahedral charge (%/CEC, left y-axis) and the layer charge density (LCD in eq/FU, right y-axis).

https://doi.org/10.1346/CCMN.2016.064041 Published online by Cambridge University Press

the CEC was determined before and after this treatment to measure the tetrahedral charge (autocorrelation). The scatter of the data in the curve of Figure 2a, therefore, reflects the reproducibility of the method. Interestingly, the same trend was observed for the Mg-saturated samples (Figure 2b) despite a lower CEC decrease (7−36 meq/100 g, Table 3) in comparison to the Li-saturated samples (27−70 meq/100 g, Table 3). A larger CEC drop was found for the samples with a low tetrahedral charge and samples with a high tetrahedral charge showed a lower CEC decrease. This suggests that the octahedral charge is important with respect to the fixation mechanism. Such a relation could hardly be explained if Mg remained at the bottom of the hexagonal holes, which should not be affected by the charge location. For both the Li and Mg sample series, no relationship with the layer charge density was found ($R^2 = 0.1$).

A temperature of 250ºC is not expected to occur in either a large scale HLRW deposition test or in any bentonite-based disposal concept (Dohrmann *et al*., 2013a). Heating up to 120ºC in order to extrapolate mineral reactions that occur over large time scales at lower temperatures (compare to Karnland *et al*., 2009) is more relevant (Figure 3). The extent of the CEC decrease in Li-saturated samples after heating at only 120ºC was much less pronounced in comparison to samples heated at 250ºC. A CEC decrease of only 1−12 meq/100 g was produced by a 120ºC heat treatment instead of the 27−70 meq/100 g decrease produced by 250ºC heat treatment (Table 3) and the CEC decrease in materials with a high tetrahedral charge was even less. This trend suggests that fixation of exchangeable cations in octahedral sites may already produce a CEC decrease despite a temperature lower than 250ºC. This CEC decrease could possibly also occur for the Mg-saturated samples (Figure 3b). In the case of the Mg-saturated samples that were heated to 120ºC, however, the small CEC decrease was within the precision limits of the method, which was about ±1−2 meq/100 g (Dohrmann *et al*., 2012) and explains the "negative" CEC difference values (Figure 3b). These results only allow a tentative conclusion because the differences were rather small (at the detection limit). The CEC differences for samples with a high tetrahedral charge ranged from −1 to +1 meq/100 g, which is within the precision of the method. The differences in the CECs of the samples with predominantly octahedral charge, on the other hand, ranged from 1−4 meq/100 g). Prolonged heating at 120ºC would probably increase this effect. The large scale *in situ* tests ran about 10−50 times longer and for part of the time at even slightly higher temperatures and both factors might have promoted dioctahedral to trioctahedral transformation and Mg fixation. From these results, one could expect Mg addition to octahedral vacancies as a possible reaction mechanism and explanation for the observed dioctahedral to trioctahedral transformation and Mg fixation. In reality, however, water will be present in the large scale tests. Results of the heat treatment of Li- and Mg-saturated samples in the presence of water did not show any trend towards dioctahedral to trioctahedral transformation and Mg fixation (Figure 4a,b). Even the Li, which was used to indicate what can happen with Mg in the long run, did not enter the octahedral vacancies. The reason is probably due to the hydration energy which has to be overcome before Li or Mg can enter the vacancies. The results prove that dry conditions are necessary for dioctahedral to trioctahedral transformation and Mg fixation as a solid state reaction. This result explains why dioctahedral to trioctahedral transformation and Mg fixation in the large scale tests was only observed at the very contacts of the bentonite with the metal surface of the heater. At a 1 cm distance away from the large-scale test heater surfaces, no dioctahedral to trioctahedral transformation or Mg fixa-

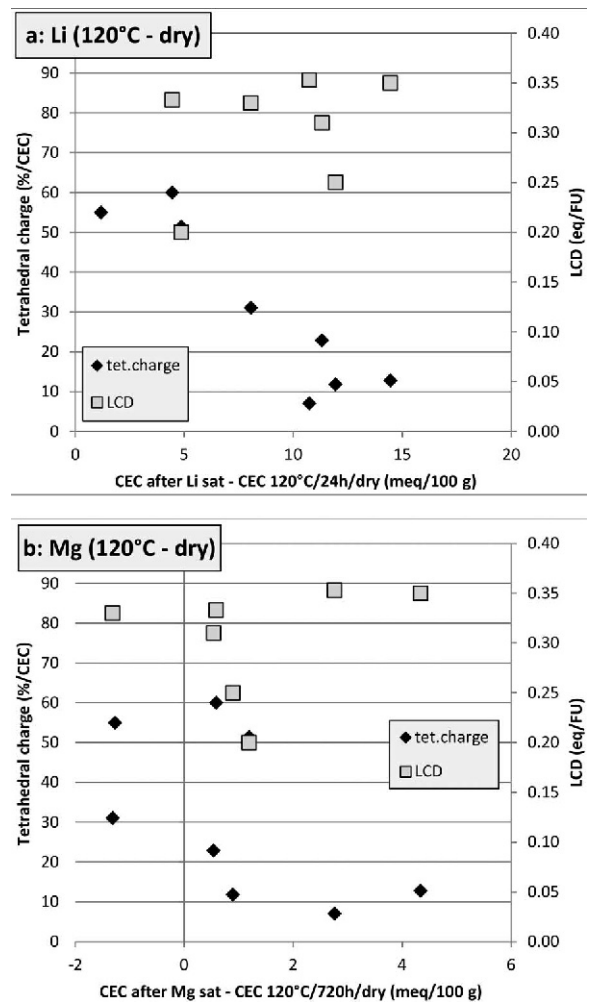

Figure 3. The CEC decrease for Li-saturated (a: series 3, Table 2) and Mg-saturated (b: series 6, Table 2) and heat treated (120ºC, dry) bentonite samples compared with the tetrahedral charge (%/CEC, left *y* axis) and the layer charge density (LCD, right *y* axis).

https://doi.org/10.1346/CCMN.2016.064041 Published online by Cambridge University Press

tion was observed, although the temperature did not differ significantly from that at the heater surface and the Mg abundance was at least slightly higher than in the reference bentonites. The Mg fixation could also be explained by alternating wet and dry conditions, but such conditions have not been observed in large scale disposal tests which are commonly monitored using a significant set of humidity sensors.

XRD

The d_{060} reflection is used to distinguish trioctahedral from dioctahedral clay minerals, giving a peak position of 1.49 Å for dioctahedral smectites and 1.53 Å for trioctahedral smectites. The samples with the largest CEC decrease (Table 3) were investigated using XRD (Figure 5). After Mg-saturation and heat treatment (series 5), a slight shift of the d_{060} peak (0.0019 to 0.0026 Å increase) was observed along with a CEC decrease of 26–36 meq/100 g. The products of heating Mg-saturated bentonites were far from pure trioctahedral minerals, but the small d_{060} peak shift pointed towards a small but increased number of trioctahedral domains in the products. The d_{060} peak was broad and, hence, determination of the peak position with a high accuracy was difficult. Results were given using 4 digits because the peak shifts were rather small and were close to the detection limit. A trend, however, could still be observed.

IR

The IR spectra of the four samples with the largest CEC decrease before (black, bottom spectrum) and after Li saturation (red, second spectrum grayscale), Mg-saturation (blue, top spectrum grayscale), and heat treatment at 250ºC (Figure 6) revealed two new bands (at about 3666 cm^{-1} and 1130 cm^{-1}) in the Li saturated bentonite B2 sample after heating to 250ºC. The peak at

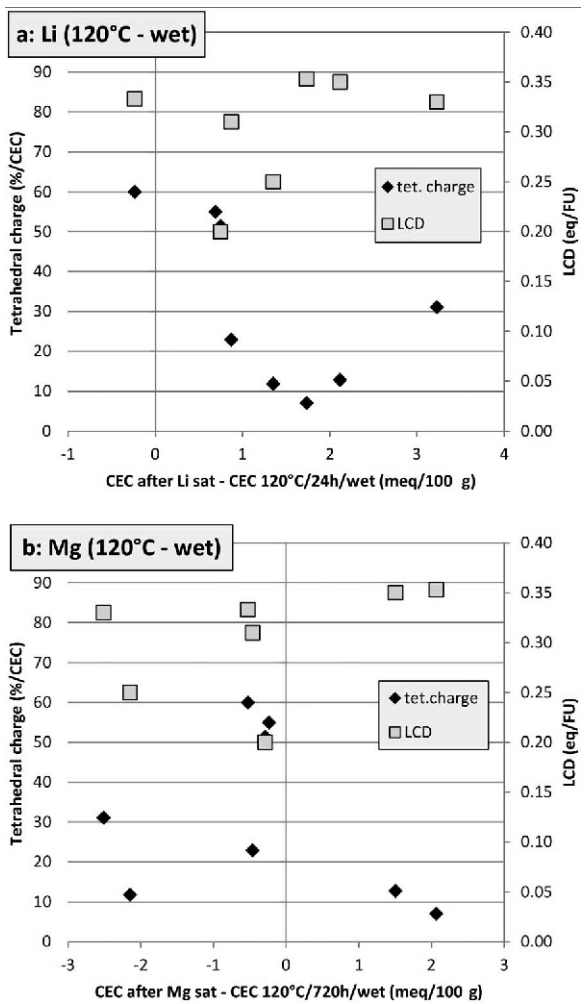

Figure 4. The CEC decrease for Li-saturated (a: series 4, Table 2) and Mg-saturated (b: series 7, Table 2) and heat treated (120ºC, wet) bentonite samples compared with the tetrahedral charge (%/CEC, left *y* axis) and the layer charge density (LCD in eq/FU, right *y* axis).

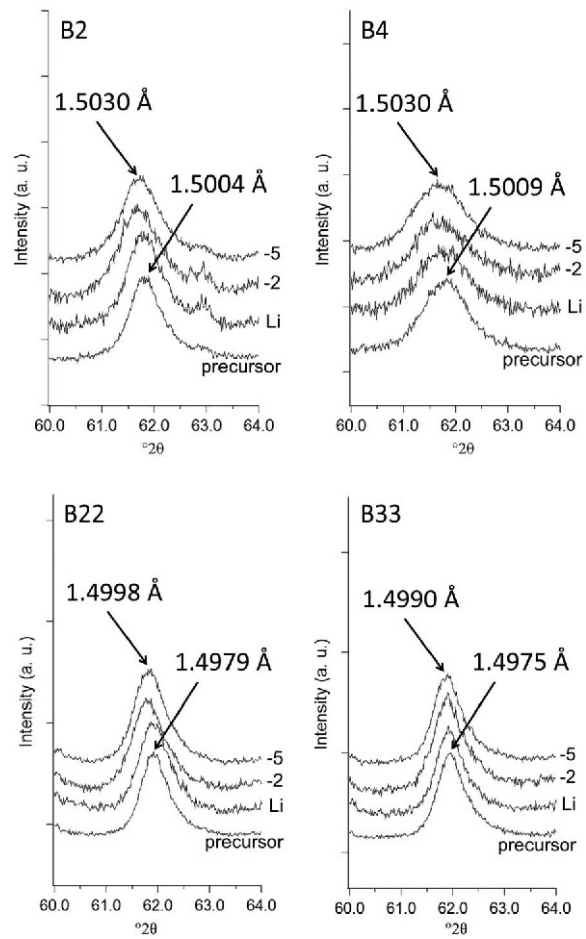

Figure 5. XRD patterns in the range 60–64º2θ showing the d_{060} reflections of four bentonite samples. The bottom to top order of the XRD patterns in the stacked patterns is as follows: precursor (untreated, Li-saturated), series 2 (Li-saturated, heated to 250ºC), series 5 (Mg-saturated, heated to 250ºC).

https://doi.org/10.1346/CCMN.2016.064041 Published online by Cambridge University Press

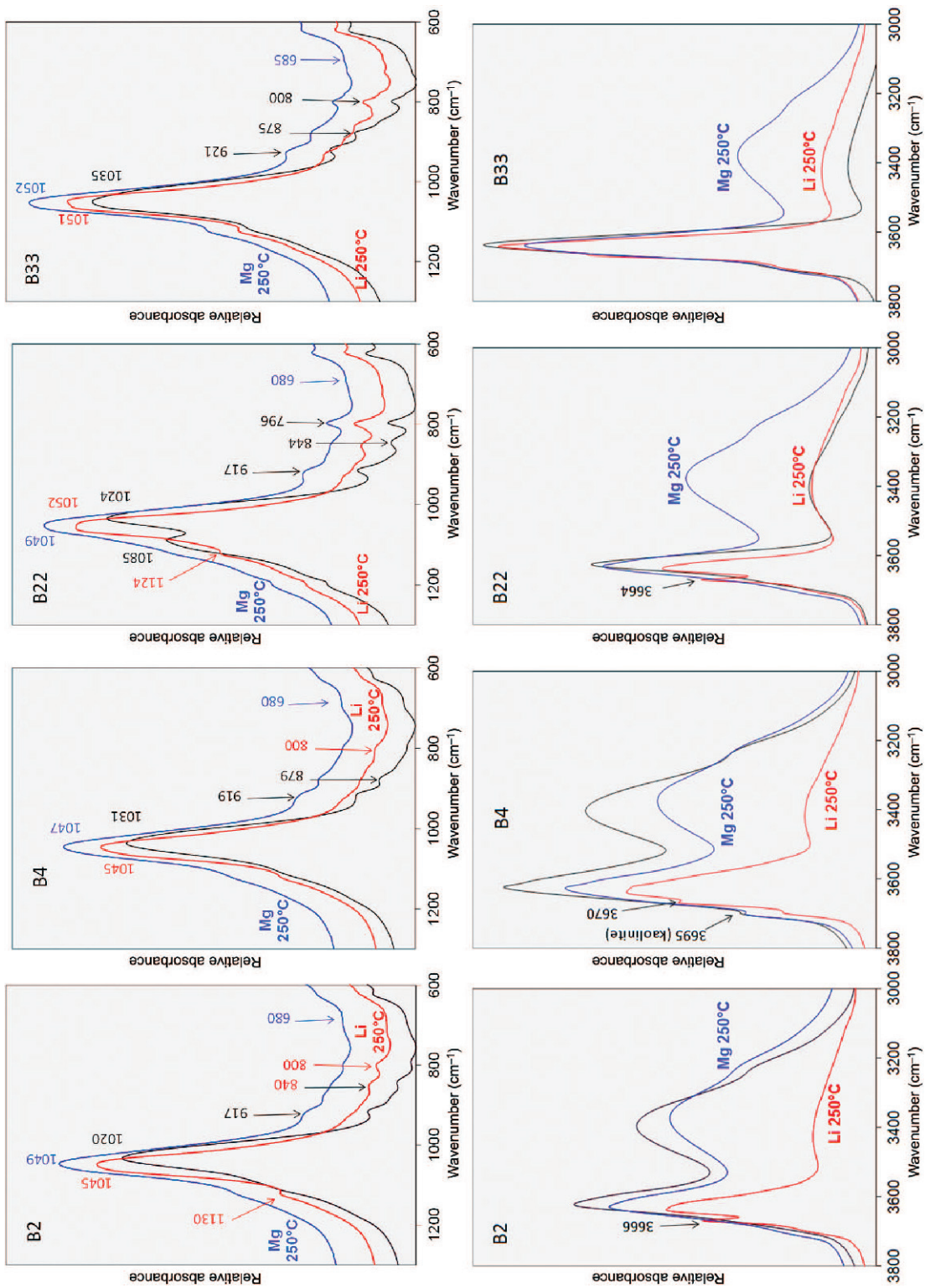

Figure 6. IR spectra (OH stretching and deformation regions) of bentonite samples: precursor (untreated bentonite, black line), Li-saturated and heated to 250°C (Li 250°C red line, light-gray grayscale), and Mg-saturated and heated to 250°C (Mg 250°C blue line, dark-gray grayscale).

https://doi.org/10.1346/CCMN.2016.064041 Published online by Cambridge University Press

3666 cm^{-1} was assigned to the AlMgLiOH stretching mode, thus indicating Li in the octahedral sheet (Calvet and Prost, 1971; Madejová et al., 1996). This band was not observed for the Mg-saturated B2 sample which does not point to any specific location for the Mg because the AlMgMgOH band would not lead to such a significant shift in band position as Li. The AlMgLiOH band was also observed for sample B22, but not for the other samples. Both of these samples had the largest CEC decreases and, hence, provided a consistent result for Li saturation and 250ºC heat treatment. Less information concerning Mg-fixation can be gained from the OH-stretching region.

The other new band observed in the Li-saturated B2 samples was at 1130 cm^{-1} and was assigned to a pyrophyllite-like structure or domains (Madejová *et al*., 1996). The other bentonite samples also had a shoulder in the 1130 cm^{-1} range.

Significant changes were observed in the position of the SiO-stretching band for both the Li- and Mg-saturated B2 samples, with shifts from 1020 to 1045 and 1049 cm^{-1}. These shifts can be explained by the effect of cations in the pseduohexagonal holes on the tetrahedral sheet (Madejová *et al*., 1996).

The OH-deformation region provides more information with respect to Li and Mg-fixation. The Li-saturated B2 sample showed an increase in the intensity of the 800 cm^{-1} band, which was previously described for Li-saturated and heated samples (Madejová *et al*., 2000). At the same time, the AlAlOH band around 915 cm^{-1} decreased in intensity. For the Mg-saturated and heated B2 samples, more diffuse bands were observed both in the MgMgMgOH region (680 cm^{-1}) and in the AlMgOH deformation region (around 845 cm^{-1}), which indicated that the octahedral bands were affected by the Mg saturation and heat treatment. These bands, however, fail to offer sufficient evidence to reach an unambiguous conclusion as to whether or not the Mg actually entered the octahedral sheet. Similar changes were observed in the SiO-stretching and OH-deformation region of the other bentonite samples. The spectrum of sample B22 was also affected by the cristobalite bands at 1085 and 796 cm^{-1}.

SUMMARY AND CONCLUSIONS

Li- and Mg-saturated samples were heated to investigate possible similarities in Li and Mg cation fixation processes. In the case of Li, most studies have concluded that it can migrate into octahedral vacancy sites that are probably near to the permanent charge. Not all vacancies may be near a permanent octahedral charge site. Those which are near charge sites may be occupied preferentially by either Li or Mg. The driving force for Li to enter the octahedral sheet is neutralization of the permanent charge in the octahedral sheet. The permanent layer charge, therefore, was reduced to a larger extent for smectites with a larger octahedral/tetrahedral charge ratio. The prerequisite for charge reduction, however, was dry conditions. Despite the low hydration energy of Li, dry conditions are required for the Li to enter the octahedral sheet where new trioctahedral bonds form, as demonstrated and confirmed by IR-spectroscopy. It is more difficult for divalent cations to enter the octahedral sheet (*e.g.* Madejová *et al*., 1999) and some doubt exists as to whether or not Mg can enter the octahedral vacancies at all. In the present study, a similar relationship between CEC reduction and the initial octahedral/tetrahedral charge were found for Li- and Mg-saturated and heated bentonites. This finding in the present study supports the view that Mg can also enter at least some octahedral vacancies, although Mg has a higher hydration energy and slightly larger radius than Li. Measurements using X-ray diffraction indicated a slight shift of the d_{060} reflection towards that of trioctahedral smectites. IR-spectroscopy showed some changes in the OH-deformation region which, however, cannot be interpreted unambiguously. The strongest indication that Mg was able to reach at least some octahedral vacancies resulted from the similar relationship between CEC reduction and the initial octahedral/tetrahedral charge ratio. By entering the bottom of the pseudohexagonal holes, charge reduction should also be possible even if the source of the charge is in the tetrahedral sheet. Mg migration into the octahedral vacancies would explain (1) why trioctahedral domains were clearly found at the interface between heated metal surfaces and bentonites in large scale HLRW tests and (2) why this reaction was restricted to the contact surface, which must have been locally dry.

The phenomenon of Mg enrichment near the surface of a metal heater can be explained based on the results of the present study. This explanation is independent of the actual location of Mg fixation in smectite structures. The basis for the explanation is that dry conditions lead to Mg fixation in the smectite (either in the octahedral sheet or in the pseudohexagonal holes). The incorporation of Mg into the smectite structure near a heated metal surface represents a chemical sink. The Mg concentration in the pore water is reduced and more Mg is transported from outer parts towards the regions were Mg had been removed by the smectite. This would lead to an increase of total Mg content near the heated metal surface. Cation exchange processes, however, may also be relevant and dissolution/precipitation processes cannot be ruled out.

REFERENCES

Calvet, R. and Prost, R. (1971) Cation migration into empty octahedral sites and surface properties of clays. *Clays and Clay Minerals*, **19**, 175–186.

Dohrmann, R. (2006) Problems in CEC determination of calcareous clayey sediments using the ammonium acetate method. *Journal of Plant Nutrition and Soil Science*, **169**, 330–334.

Dohrmann, R. and Kaufhold, S. (2009) Three new, quick CEC

https://doi.org/10.1346/CCMN.2016.064041 Published online by Cambridge University Press

methods for determining the amounts of exchangeable calcium cations in calcareous clays. *Clays and Clay Minerals*, **57**, 338–352.

Dohrmann, R. and Kaufhold, S. (2014) Cation exchange and mineral reactions observed in MX 80 buffers samples of the prototype repository in situ experiment in Äspö, Sweden. *Clays and Clay Minerals*, **62**, 357–373.

Dohrmann, R., Genske, D., Karnland, O., Kaufhold, S., Kiviranta, L., Olsson, S., Plötze, M., Sandén, T., Sellin, P., Svensson, D., and Valter, M. (2012) Interlaboratory CEC and exchangeable cation study of bentonite buffer materials: I. Cu(II)-triethylentetramine method. *Clays and Clay Minerals*, **60**, 162–175.

Dohrmann, R., Kaufhold, S., and Lundqvist, B. (2013a) The role of clays for safe storage of nuclear waste. Pp. 677–710 in: *Handbook of Clay Science, Techniques and Applications* (F. Bergaya and G. Lagaly, editors). Developments in Clay Science, Vol. **5B**. Elsevier, Amsterdam.

Dohrmann, R., Olsson, S., Kaufhold, S., and Sellin, P. (2013b) Mineralogical investigations of the first package of the alternative buffer material test – II. Exchangeable cation population rearrangement. *Clay Minerals*, **48**, 215–233.

Greene-Kelly, R. (1952) A test for montmorillonite. *Nature*, **170**, 1130–1131.

Hofmann, U. and Klemen, R. (1950) Verlust der Austauschfähigkeit von Lithiumionen an Bentonit durch Erhitzung. *Zeitschrift für anorganische und allgemeine Chemie*, **262**, 95–99.

Hrobáriková, J., Madejová, J., and Komadel, P. (2001) Effect of heating temperature on Li-fixation, layer charge and properties of fine fractions of bentonites. *Journal Material Chemistry*, **11**, 1452–1457.

Jaynes, W.F. and Bigham, J.M. (1987) Charge reduction, octahedral charge, and lithium retention in heated, Li-saturated smectites. *Clays and Clay Minerals*, **35**, 440–448.

Jaynes, W.F., Traina, S.J., Bigham, J.M., and Johnston, C.T. (1992) Preparation and characterization of reduced-charge hectorites. *Clays and Clay Minerals*, **40**, 397–404.

Kaufhold, S. and Dohrmann, R. (2008) Detachment of colloidal particles from bentonites in water. *Applied Clay Science*, **39**, 50–59.

Kaufhold, S. and Dohrmann, R. (2009) Mineralogical and geochemical alteration of the MX80 bentonite from the LOT experiment characterization of the A2 parcel. Pp. 225–250 in: *Long Term Test of Buffer Material at the Äspö Hard Rock Laboratory* (O. Karnland, S. Olsson, A. Dueck, M. Birgersson, U. Nilsson, T. Hernan-Håkansson, K. Pedersen, S. Nilsson, T.E. Eriksen, and B. Rosborg, editors). LOT project, Final report on the A2 test parcel, TR-09-29, ISSN 1404-0344.

Kaufhold, S. and Dohrmann, R. (2010) Effect of extensive drying on the cation exchange capacity of bentonites. *Clay Minerals*, **45**, 441–448.

Kaufhold, S. and Dohrmann, R. (2016) Distinguishing between more and less suitable bentonites for storage of high-level radioactive waste. *Clay Minerals*, **51**, 289–302.

Kaufhold, S., Dohrmann, R., Koch, D., and Houben, G. (2008) The pH of aqueous bentonite suspensions. *Clays and Clay Minerals*, **56**, 338–343.

Kaufhold, S., Dohrmann, R., and Klinkenberg, M. (2010a) Water uptake capacity of bentonites. *Clays and Clay Minerals*, **58**, 37–43.

Kaufhold, S., Dohrmann, R., Klinkenberg, M., Siegesmund, S., and Ufer, K. (2010b) N_2-BET specific surface area of bentonites. *Journal of Colloid and Interface Science*, **349**, 275–282.

Kaufhold S., Hein, M., Dohrmann, R., and Ufer, K. (2012) Quantification of the mineralogical composition of clays using FTIR spectroscopy. *Journal of Vibrational Spectroscopy*, **59**, 29–39.

Kaufhold, S., Dohrmann, R., Sandén, T., Sellin, P., and Svensson, D. (2013) Mineralogical investigations of the alternative buffer material test – I. Alteration of bentonites. *Clay Minerals*, **48**, 199–213.

Kaufhold, S., Sanders, D., Dohrmann, R., and Hassel, A.-W. (2015) Fe corrosion in contact with bentonites. *Journal of Hazardous Materials*, **285**, 464–473.

Karakassides, M.A., Gournis, D., and Petridis, D. (1999) An infrared reflectance study of Si-O vibrations in thermally treated alkali-saturated montmorillonites. *Clay Minerals*, **34**, 429–438.

Karnland, O., Olsson, S., Dueck, A., Birgersson, M., Nilsson, U., Hernan-Håkansson, T., Pedersen, K., Nilsson, S., Eriksen, T.E., and Rosborg, B. (2009) Long term test of buffer material at the Äspö Hard Rock Laboratory, LOT project, *Final report on the A2 test parcel*, TR-09-29, ISSN 1404-0344

Madejová J., Bujdak J., Gates W.P., and Komadel P. (1996) Preparation and infrared spectroscopic characterization of reduced-charge montmorillonite with various Li contents. *Clay Minerals*, **31**, 233–241.

Madejová, J., Bujdák, J., Petit, S., and Komadel, P. (2000) Effects of chemical composition and temperature of heating on the infrared spectra of Li-saturated dioctahedral smectites. (I) Mid-infrared region. *Clay Minerals*, **35**, 739–751.

Meier, L.P. and Kahr, G. (1999) Determination of the cation exchange capacity (CEC) of clay minerals using the complexes of Copper(II) ion with triethylenetetramine and tetraethylenepentamine. *Clays and Clay Minerals*, **47**, 386–388.

Perronnet, M., Villiéras, F., Jullien, M., Razafitianamaharavo, A., Raynal, J., and Bonnin, D. (2007) Towards a link between the energetic heterogeneities of the edge faces of smectites and their stability in the context of metallic corrosion. *Geochimica et Cosmochimica Acta*, **71**, 1463–1479.

Plötze, M., Kahr, G., Dohrmann, R., and Weber, H. (2007) Hydro-mechanical, geochemical and mineralogical characteristics of the bentonite buffer in a heater experiment. The HE-B project at the Mont Terri rock laboratory. *Physics and Chemistry of the Earth*, **32**, 730–740.

Savage, D., Bateman, K., Hill, P., Hughes, C., Milodowski, A., Pearce, J., Rae, E., and Rochelle, C. (1992) Rate and mechanism of the reaction of silicates with cement pore fluids. *Applied Clay Science*, **7**, 33–45.

Savage, D., Watsona, C., Benbow, S., and Wilson, J. (2010) Modelling iron–bentonite interactions. *Applied Clay Science*, **47**, 91–98.

Srasra, E., Bergaya, F., and Fripiat, J.J. (1994) Infrared spectroscopy study of tetrahedral and octahedral substitutions in an interstratified illite-smectite clay. *Clays and Clay Minerals*, **42**, 237–241.

Stackhouse, S. and Coveney, P.V. (2002) Study of thermally treated lithium montmorillonite by ab initio methods. *Journal of Physical Chemistry B*, **106**, 12470–12477. doi: 10.1021/jp025883q.

Steudel, A., Heinzmann, R., Indris, S., and Emmerich, K. (2015) CEC and ^{7}Li MAS NMR study of the interlayer Li+ in the montmorillonite-beidellite series at room temperature and after heating. *Clays and Clay Minerals*, **63**, 337–350.

Svensson, D. (2015) Saponite formation in the ABM2 iron-bentonite field experiment at Äspö hard rock laboratory, Sweden. Pp. 168–169 in: *Clays in Natural and Engineered Barriers for Radioactive Waste Confinement*, Sixth International Meeting, Program & Abstracts, Brussels.

(*Received 28 April 2016; revised 6 December 2016; Ms. 1104; AE: P. Ryan*)